Heinrich Garn*, Bernhard Kohn, Christoph Wiesmeyr, Klaus Dittrich, Markus Wimmer, Magdalena Mandl, Gerhard Kloesch, Marion Boeck, Andrijana Stefanic and Stefan Seidel

3D detection of the central sleep apnoea syndrome

Abstract: In polysomnography, an oronasal thermal airflow sensor and respiratory inductance plethysmography (RIP) belts at thorax and abdomen are used to detect central sleep apnoea. These sensors are uncomfortable to wear, can disturb the patient´s sleep, and data quality can be significantly diminished if a sensor slips off the patient. Contactless measurements would be a desirable alternative. We utilized a 3D time-of-flight sensor to monitor respiratory-related chest movements to decipher epochs of normal breathing and apnoea in ten adult patients with a total of 467 apnoea events. Time-synchronized comparisons of 3D measurements of chest movements due to respiration to polysomnography signals from rip belts and nasal airflow proved that the 3D sensor provided largely equivalent results. This new technique could support the diagnosis of central sleep apnoea and Cheyne-Stokes respiration.

Keywords: 3D, central sleep apnoea, Cheyne-Stokes breathing.

https://doi.org/10.1515/cdbme-2017-0174

***Corresponding author: Heinrich Garn:** AIT Austrian Institute of Technology GmbH, Donau-City-Strasse 1, A-1220 Vienna, Austria, e-mail: Heinrich.garn@ait.ac.at
Bernhard Kohn, Christoph Wiesmeyr, Klaus Dittrich: AIT Austrian Institute of Technology GmbH, Donau-City-Strasse 1, A-1220 Wien, Austria
Markus Wimmer, Magdalena Mandl: Kepler University Clinic, Department of Neurology 2, Krankenhausstrasse 9, A-4021 Linz, Austria
Gerhard Kloesch, Marion Boeck, Andrijana Stefanic, Stefan Seidel: Medical University of Vienna, Department of Neurology, Waehringer Guertel 18-20, 1090 Wien, Austria

1 Introduction

The central sleep apnoea syndrome [1] is characterized by a cessation or decrease of ventilatory effort during sleep. The breathing effort is diminished or absent for typically 10 to 30 seconds. It is usually associated with blood oxygen desaturation and increased carbon dioxide. The body can react with an arousal, increasing e.g. the heart rate. Frequent arousals or awakenings can cause non-restorative sleep and daytime sleepiness. The hemodynamic complications of this syndrome include the development of systemic hypertension, cardiac arrhythmias, pulmonary hypertension, and cardiac failure [1].

Cheyne–Stokes respiration is characterized by progressively deeper and sometimes faster breathing, followed by a gradual decrease that results in an apnoea. The crescendo-diminuendo pattern repeats, associated with changing serum partial pressures of oxygen and carbon dioxide. Possible causes are chronic heart failure or damage to respiratory centres.

2 Methods for sleep apnoea detection

2.1 Scoring rules

According to the AASM scoring guide [2], “An apnea shall be scored if there is a drop in the peak signal excursion by ≥ 90 % of the pre-event baseline. The duration of the ≥ 90 % drop in the sensor signal must be ≥ 10 seconds.” Events shall be classified as being obstructive (“associated with continued or increased inspiratory effort through-out the entire period of absent airflow”), central (“associated with absent inspiratory effort through-out the entire period of absent airflow”) or mixed. For identification of an apnoea during a diagnostic study, an oronasal airflow sensor shall be used. For identification of a hypopnoea, a nasal pressure transducer is fore-

seen. However, both kinds of sensors are allowed as respective alternatives.

2.2 Measurement alternatives using optical sensing

Video-based methods for automatic detections of chest movements have been described in some studies, but are not established yet.

2.2.1 2D video image processing

Using three near-infrared grey scale cameras, Wang et al. [3] monitored breathing behaviour and detected subtle, cyclical breathing signals. A self-adaptive breathing template and a robust action classification method were used to recognize abnormal breathing activities. An accuracy of 94 % was reported.

Bennett et al. [4] showed that a thermal camera can be used for the detection of breathing behaviour via of subtle colour variations due to inspiratory and expiratory airflow in the region of the nose. There was no quantitative evaluation of detection rates.

2.2.2 3D image processing using time-of-flight sensors

Falie et al. [5] and Falie & Ichim [6] used novel time-of-flight (TOF) sensors to detect obstructive sleep apnoea from phase differences between signals from thorax and abdomen. Quantitative evaluations of detection rates were not reported.

Kohli & Shotton [7] gave an overview of the developments in human pose detection using time-of-flight cameras.

3 Method for 3D detection of the central sleep apnoea syndrome

3.1 Measurement equipment

We used a time-of-flight sensor (MS Kinect One) for measuring chest movements due to respiration. The TOF sensor transmits 30 invisible near-infrared light pulses (860 nanometres) per second onto the person lying in bed. The reflected light is measured by 512 x 424 pixels, providing sufficient resolution for identifying chest movements at thorax and abdomen. Each pixel provides a grey scale value (derived from signal intensity) and a distance value (computed from the time-of-flight) [8, 9]. **Figure 1** shows the setup in the sleep laboratory.

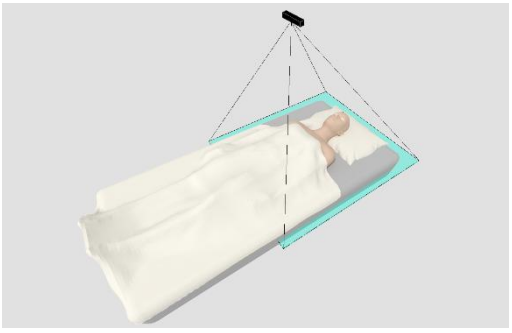

Figure 1: Setup for 3D measurements of breathing motion

3.2 Determination of respiratory effort

The respiratory effort was derived from the region of maximal variation in the measured distance. As sleeping persons will change their position in the bed and turn from one side to the other, the locations of the chest can also change. Therefore, we applied continuous monitoring of the time courses of the distance values of all pixels. Their variation was the characteristic feature for determining respiratory effort. It turned out that it showed a similar time course as the signals provided by the RIP belts. Comparison of this feature between periods with and without breathing revealed quantitative criteria for automatic detection of relevant reductions in respiratory effort. **Figure 2** shows an example of the raw 3D signal of a central apnoea. For further processing, a window low pass filter of 40 frames and temporary de-trending were applied to minimize noise.

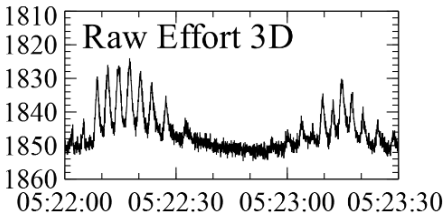

Figure 2: Illustration of a raw respiratory effort signal derived from 3D chest movement during a central apnea event

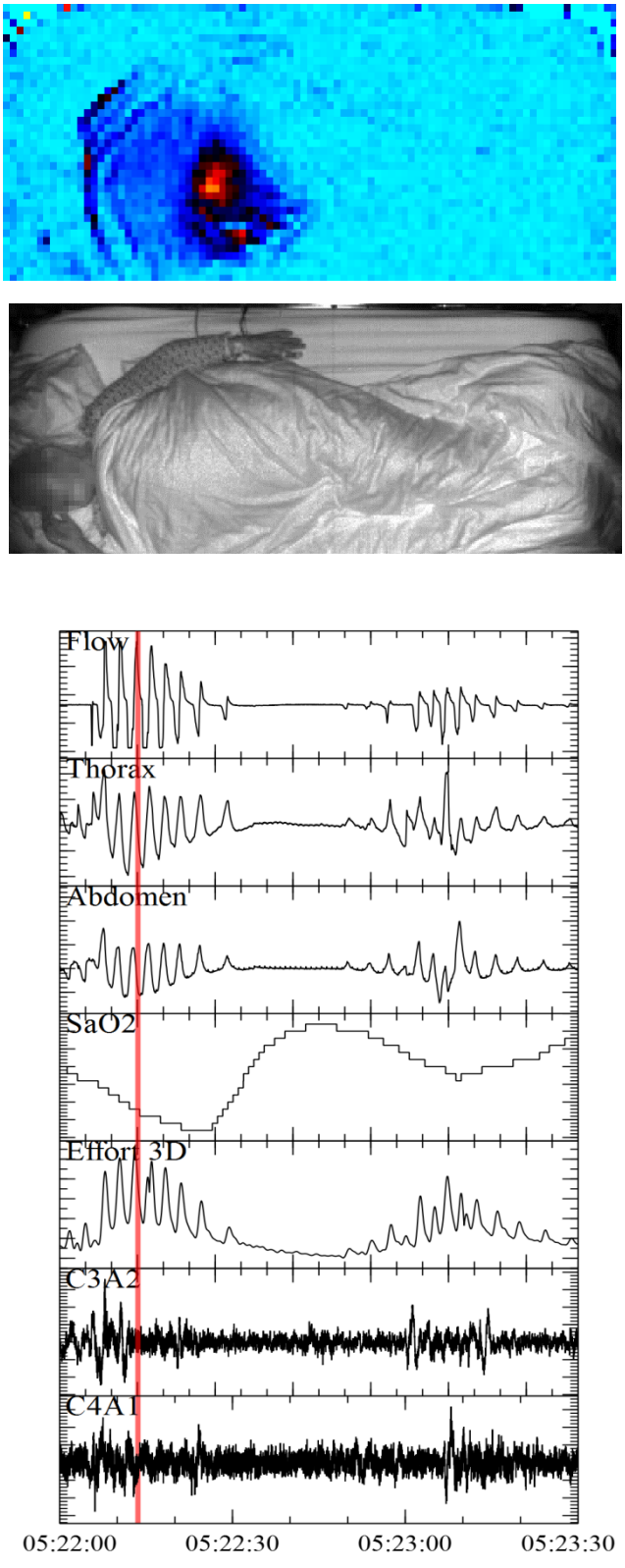

Figure 3: Setup for 3D measurements of breathing motion

Figure 3 shows the method of comparing PSG signals from the oronasal airflow sensor, RIP belts at thorax and abdomen, oxygen, and EEG to the 3D measurements of chest movements. The upper image represents the grey scale near infrared video. The figure below visualises the amount of motion via colour codes (red and yellow indicate motion, blue indicates no motion). The signal traces below show the time-synchronised comparison of the amount of 3D effort computed from the depth map to the PSG signals during a period with central apnoea.

3.3 Patients

We performed assessments with 10 adult patients (6 males aged 19-74 years (45.6±27.5) and 4 females aged 36-84 years (60±24)) from the clinical routine of the sleep laboratories of the Department of Neurology of the Medical University of Vienna and the Department of Neurology 2 of the Kepler University Hospital in Linz in the frame of a clinical study that was approved by the competent ethics committees (Medical Univ. of Vienna, State of Upper Austria). Patients underwent full-night polysomnography with additional 3D recording.

3.4 Experimental validation

Purpose of the experimental study was to evaluate the coincidence of central apnoea detected in 3D and in PSG. For this purpose, the clocks of the PSG computer and the computer acquiring the 3D signals were time synchronized via a sync signal that was fed into the PSG head box. Recorded files were copied from both systems in .edf format and processed by the AIT Annotator© program.

First of all, the positions of the apnoea were identified by visual inspection of the airflow signal according to the AASM scoring rules [2]. Then, these events were manually classified as being obstructive, central or mixed on the basis of (a) the RIP belt signals from thorax and abdomen and (b) the 3D respiratory effort signal. As the 3D respiratory effort signal and the RIP belt signals relate to the same physical motion of the chest, the classification process was applied in the same way.

4 Results

We identified a total of 467 apnoea events in the polysomnography recordings based on oronasal airflow. Comparing the results of the analysis of the RIP belt signals to the results of

the 3D effort analysis revealed 441 (94 %) respiratory events where both methods led to the same classification result. There were five patients with central apnoea. For patient no. 4, the 3D method identified twice as much central apnoea than the PSG. Visual inspection of the video recordings revealed that the chest movements were so weak that they could be detected by the sensitive RIP belts, but largely hidden under the blanket so that the 3D system did not detect it. Overall, coincidences between 67 % and 100 % were achieved, corresponding to 94 % on average. **Table 1** summarizes these results.

Cheyne-Stokes respiration was found in only one patient. The time courses of the respiration from 3D and thorax/abdomen were equivalent.

Table 1: Comparison between 3D effort and RIP belt signals.

Pat. No.		3D effort			RIP belt			Coincidence
	Tot	OA	CA	MA	OA	CA	MA	
1	51	50	**0**	1	51	**0**	0	98%
2	19	9	**5**	5	9	**4**	6	95%
3	17	16	**0**	1	17	**0**	0	94%
4	49	27	**16**	6	37	**8**	4	78%
5	227	219	**0**	8	219	**0**	8	100%
6	50	8	**39**	3	11	**33**	6	88%
7	6	4	**2**	0	6	**0**	0	67%
8	22	22	**0**	0	22	**0**	0	100%
9	11	2	**0**	9	4	**0**	7	82%
10	15	2	**12**	1	3	**12**	0	87%
	467	**359**	**74**	**34**	**379**	**57**	**31**	**94%**

OA: obstructive apnoea; CA: central apnoea; MA: mixed apnoea

5 Discussion and conclusion

The comparison of apnoea classifications derived from RIP belt signals and from 3D analysis revealed differences between 0 % and 33 %, depending on the patient. The 3D system detected more central and less obstructive apnoea. The false positives could be due to the threshold that was set for motion detection: The criterion of “absent inspiratory effort” [2] does not include a quantitative limit. Adaptive thresholds will be used in the future to account for individual signal amplitudes.

In clinical routine, misclassification of obstructive events as central could also occur if the chest and abdominal effort belts were not tightened properly and if they were not placed in positions of maximum movement during respiration. Even when calibrated, RIP may falsely classify events as being central, as it may not detect feeble respiratory effort in up to 9 % of patients [10].

Using contactless sensing offers some substantial advantages over body-mounted sensors:

- Body-mounted sensors can disturb the patient´s sleep. Any sensor that can be applied without body contact enhances patient comfort.
- In clinical practice, RIP belts tend to get out of place or come off during the night. The assistant has to re-adjust it (which will likely wake up the patient) or leave it as it is (making the recording unusable). In any case, a contactless sensor will provide constant, better data quality.
- Mounting, re-adjusting and removing body-worn sensors means personnel effort, which can be saved by using a contactless sensor.

The 3D-based method could be applicable in ambulant settings and home monitoring, providing an efficient way for pre-screening.

Author’s Statement

Research funding: The authors state no funding involved. Conflict of interest: Authors state no conflict of interest. Informed consent: Informed consent has been obtained from all individuals included in this study. Ethical approval: The research related to human use complies with all the relevant national regulations, institutional policies and was performed in accordance with the tenets of the Helsinki Declaration, and has been approved by the authors' institutional review board or equivalent committee.

References

[1] The International Classification of Sleep Disorders – Third Edition (ICSD-3). American Academy of Sleep Medicine 2014.

[2] Berry RB, Brooks R, Gamaldo CE, Harding SM, Lloyd RM et al. The AASM Manual for the Scoring of Sleep and Associated Events, Version 2.4. American Academy of Sleep Medicine 2017.

[3] Wang CW, Hunter A, Gravill N et al. Unconstrained Video Monitoring of Breathing Behavior and Application to Diagnosis of Sleep Apnea. IEEE Trans. Biomedical Engin. 2014; 61(2):396-404.

[4] Bennett SL, Goubran R, Knoefel F. The Detection of Breathing Behavior Using Eulerian-Enhanced Thermal Video. IEEE

International Conference Engineering in Medicine and Biology 2015; Proc. pp. 7474-7477.
[5] Falie D, David L, Ichim M. Statistical algorithm for detection and screening sleep apnea. International Symposium on Signals, Circuits and Systems 2009; Proc. pp. 1-4.
[6] Falie D, Ichim M. Sleep monitoring and sleep apnea event detection using a 3D camera. International Conference on Communications 2010; Proc. pp. 177-180.
Kohli P, Shotton J. Key Developments in Human Pose Estimation for Kinect. Consumer Depth Cameras for Computer Vision. Springer London 2013.
[7] Schwarte R. Dynamic 3D-Vision. Proceedings IEEE International Symposium on Electron Devices for Microwave and Optoelectronic Applications 2001, proc. 241-248.
[8] Payne A, Daniel A, Mehta A et al. A 512×424 CMOS 3D Time-of-Flight Image Sensor with Multi-Frequency Photo-Demodulation up to 130MHz and 2GS/s ADC. 2014 IEEE International Solid-State Circuits Conference; Proc. pp. 134-136.
[9] Berry RB, Wagner MH. Sleep Medicine Pearls, Third edition, chapter 13. Elsevier Saunders, Philadelphia 2015.